Preparation and Properties of Naringin Epoxy/UiO-66 Composites

Yonggang Du (dyg2166@sina.com)
Shijiazhuang Tiedao University https://orcid.org/0000-0003-3931-3285
Gonghui Shi
Shijiazhuang Tiedao University
Hui Wang
Shijiazhuang Tiedao University
Ge Zhao
Shijiazhuang Tiedao University
Wei Li
Shijiazhuang Tiedao University
Chuanfang Liu
Shijiazhuang Tiedao University
Zilong Zhao
Shijiazhuang Tiedao University

Research Article

Keywords: Naringenin, bio-based epoxy resin, UiO-66, toughening

Posted Date: September 1st, 2021

DOI: https://doi.org/10.21203/rs.3.rs-853871/v1

Abstract

The novel bio-based epoxy resin based on naringenin was synthesized. The naringenin epoxy/UiO-66 composites were prepared by casting process with UiO-66 as modifier and maleic anhydride as curing agent. The influences of UiO-66 content on mechanical properties, thermal stability and flame retardancy of naringenin epoxy/UiO-66 composites were investigated. The results showed that the impact strength, glass transition temperature and limiting oxygen index of pure naringenin epoxy resin were 2.0 kJ/m^2, 96 °C and 1.2% higher than that of di-glycidyl ether of bisphenol A (DGEBA), respectively. UiO-66 can significantly improve the impact strength of naringenin epoxy resin while assisting improve its flame retardancy. When UiO-66 content was 4 wt%, the impact strength and limiting oxygen index of the naringenin epoxy/UiO-66 composite were 7.6 kJ/m^2 and 24.5%, which were 85.4% and 3.5% higher than that of pure naringin epoxy resin, respectively.

1 Introduction

Epoxy resin is currently the most widely used type of thermosetting polymer. Due to epoxy group has high reactivity to many functional groups (such as carboxyl, amino and hydroxyl). Therefore, epoxy resin has been widely used in adhesives, coatings, electronic packaging, construction materials, aerospace and other fields [1–3]. At present, almost 90% of the epoxy resins produced in the world is di-glycidyl ether of bisphenol A (DGEBA). DGEBA has been made by reacting bisphenol A (BPA) with epichlorohydrin. BPA is mainly derived from petrochemical resources. In addition, BPA is an endocrine disruptor which mimics estrogen and harms human health. Thus, many countries have imposed strict restrictions on the use of BPA. Exploring natural renewable resources to prepare novel bio-based epoxy resins has important scientific research and environmental protection values [4, 5].

In the past few decades, researchers have investigated a large number of bio-based raw materials and used them to prepare bio-based epoxy resins. For example, vegetable oil [6], lignin [7, 8], rosin [9–11], natural polyphenols [12, 13] and so on. Many studies have shown that bio-based epoxy resin prepared from biomass raw materials and their derivatives with rigid structure and multifunctional groups have good mechanical properties and thermal stability [14]. Naringenin is a natural flavonoid compound. Naringenin has a wide range of sources in nature. It is mainly present in the form of glycosides (naringin) in the peel and pulp of rutaceae plants such as grapefruit, orange, orange, and tomato. The condensed aromatic structure of naringin molecule makes it has good mechanical properties and thermal stability. The existence of three phenolic hydroxyl groups in the naringenin molecule makes it easy to be functionalized. Therefore, naringenin is expected to replace BPA to prepare high-performance bio-based epoxy resins.

Like petroleum-based epoxy resin, rigid bio-based epoxy resin also has the shortcomings of high brittleness and poor impact strength, which limits its application [15]. Therefore, scholars have conducted a lot of research on the toughening modification of bio-based epoxy resin in recent years. Among them, nano-modification is one of the important methods of epoxy resin toughening modification. Metal

Organic Frameworks (MOF) is an emerging nanomaterial. MOF has the advantages of high porosity, low density, large specific surface area, regular pores, adjustable pore size, diversity of topological structure and tailorability [16]. Using MOF for polymer modification can improve the mechanical properties and thermal stability of the material matrix at the same time [17]. As an important type of MOF, UiO-66 has received extensive attention due to its excellent chemical and hydrothermal stability. Liu et al. [18] used UiO-66 as a nano-filler to enhance the mechanical properties of hydrogels. Found that the polar groups and cationic metal centers on the surface of the MOF largely determine the toughening effect of the hydrogel. Chen et al. [19] used UiO-66 as a flame retardant to modify polystyrene (PS). The flame-retardant mechanism of UiO-66 on PS was to promote char formation and produce heat insulation layer.

In this work, the novel bio-based naringenin epoxy resin matrix was synthesized and UiO-66 was used as a modifier for it. The influences of UiO-66 content on mechanical properties, dynamic mechanical properties, thermal stability and flame retardancy of naringenin epoxy/UiO-66 composites were investigated. This work provides experimental and theoretical basis for the research and development of novel high-impact bio-based epoxy composite material with flame retardancy.

2 Experimental

2.1 Materials

Naringenin (supplied by Shanghai Saen Chemical Technology Co., Ltd, China), terephthalic acid (supplied by Shanghai Aladdin Biochemical Technology Co., Ltd, China), zirconium tetrachloride (supplied by Beijing Bailingwei Technology Co., Ltd, China), potassium hydrogen phthalate, concentrated hydrochloric acid, absolute ethanol, sodium chloride (supplied by Tianjin Yongda Chemical Reagent Co., Ltd, China), epichlorohydrin and sodium hydroxide (supplied by Tianjin Fuchen chemical Reagent Factory, China), N,N-Dimethylbenzylamine and maleic anhydride (supplied by MacLean Biochemical Technology co. LTD, China), acetone (supplied by Tianjin Komiou Chemical Reagent Co., Ltd, China), Cetyl Trimethyl Ammonium Bromide (supplied by Tianjin Zhiyuan Chemical Reagent Co., Ltd, China), di-glycidyl ether of bisphenol A (DGEBA, trade name E51, epoxy value is 0.51, Tianjin Tianhaoda chemical co. LTD, China).

2.2 Synthesis of naringenin epoxy resin matrix (NER)

The naringenin (0.072 mol), epichlorohydrin (1.17 mol) and hexadecyl-trimethylammonium bromide (0.0035 mol) were successively added into a 250 ml four-neck flask equipped with a magnetic stirrer, a reflux condenser and a thermometer. The mixture was heated to 100 ℃ and reacted for 6 h under stirring. After that, the mixture was cooled to 50 ℃, 0.22 mol of sodium hydroxide was gradually added to the flask and reacted at 60 ℃ for 1 h. Then the mixture was cooled to room temperature again, and washed by deionized water to neutral. The organic phase was dried by anhydrous magnesium sulfate overnight. The remaining epichlorohydrin and water were removed by a rotary evaporator and a dark brown viscous liquid was obtained. The theoretical structure of naringenin epoxy resin matrix is shown in Fig. 1.

2.3 Synthesis of UiO-66

UiO-66 was synthesized according to reference 20. Zirconium Tetrachloride ($ZrCl_4$) (0.227 mmol) and 1,4-phthalic acid (H_2BDC) (0.227 mmol) were dissolved in N, N-dimethylformamide (DMF) (340 mmol) under stirring at room temperature. Then the obtained mixture was sealed and placed in a pre-heated oven at 120 ˚C for 24 h. After cooling in air to room temperature the solid was filtered. Then the solid was washed by DMF and methanol three times, respectively. Then the product was dried to constant weight in a vacuum oven at 40 ℃. Finally, UiO-66 in powder form was obtained. The structure of UiO-66 as shown in Fig. 2.

2.4 Preparation of NER/UiO-66 composites

Maleic anhydride (MAH, dissolved in 2 ml of acetone) was used as curing agent and N, N-dimethylbenzylamine (2 drops) as the catalyst. The composition of each sample is shown in Table 1. The raw materials in various proportions were mixed evenly and dispersed in acetone, then the mixture was poured into preformed model. After that, the acetone was removed in a vacuum oven at 30 ℃ for 1 h. Then the mixture was performed at 60 ℃ for 1 h, 80 ℃ for 2 h, 150 ℃ for 3 h, and 170 ℃ for 1 h. The obtained samples were referred to as sample A0-A5, respectively.

Table 1
Compositions of different samples

Sample	NER/g	E51/g	UiO-66/g	UiO-66(wt%)	MAH/g
P	0	20.00	0	0	5.08
A0	20.00	0	0	0	6.00
A1	20.00	0	0.2630	1	6.00
A2	20.00	0	0.5307	2	6.00
A3	20.00	0	0.8043	3	6.00
A4	20.00	0	1.0830	4	6.00
A5	20.00	0	1.3686	5	6.00

DGEBA (E51) as a reference, numbered sample P. The curing process of sample P was similar with series A samples. The mixture was first treated in a vacuum oven at 45 ℃ for 1 h in order to remove acetone. After that, the mixture was performed at 80 ℃ for 2 h, 130 ℃ for 3 h, 150 ℃ for 1 h, 180 ℃ for 2 h, and 220 ℃ for 1 h.

2.5 Characterization

The infrared spectroscopy of each sample has been determined by IS50 ATR-FTIR (Thermo Fisher, Corporation, U.S.A.) using ATR annex to test in situ. X-ray diffraction has been determined by D8 ADVANCE (Bruker, Corporation, Germany). Impact strength test referred to ASTM D6110-2010 for samples preparation and testing. The impact section morphology of each sample was measured by a HITACHI

SU8010 scanning electron microscope (Hitachi, Corporation, Japan). Dynamic mechanical properties of samples were determined by DMA-8000 (PE Corporation, U.S.A.). All the samples were heated from 30 to 230°C with a heating rate of 2°C/min. The testing mode was single-cantilever vibration, and the testing frequency was 2 Hz. Thermogravimetric analysis was determined by TGA/DSC3+ (Mettler-Toledo, Corporation, Switzerland). All samples were heated from room temperature to 800 ℃ under nitrogen atmospheres with a heating rate of 20°C/min. The limiting oxygen index of each sample was determined by an FTAII oxygen index meter (RC, Corporation, U.K.) according to ASTM D2863-2008.

3 Results And Discussion

3.1 Infrared spectrum analysis

The infrared spectra of naringenin and NER are shown in Fig. 3. The characteristic peaks at 1650 cm^{-1} and 1251 cm^{-1} correspond to C-O-Ph and C-O-C, respectively. The characteristic peaks at 1750 cm^{-1} and 1605 cm^{-1} correspond to C = O and C = C, respectively. The characteristic peak at 836 cm^{-1} belong to -CH of benzene ring. Both naringenin and NER contains the characteristic peaks mentioned above. In addition, the characteristic peak of NER at 910 cm^{-1} belong to epoxy group. The hydroxyl absorption peaks of NER at 3100–3500 cm^{-1} were obviously weakened, and the peaks at 2920 cm^{-1} and 2880 cm^{-1} belongs to -CH_2- stretching vibration absorption. These indicate that the phenolic hydroxyl group of the naringenin molecule has been modified to an epoxy group. Therefore, it can be proved that NER was successfully synthesized. The epoxy value of NER was determined by hydrochloric acid-acetone titration. The measured epoxy value of naringenin epoxy resin was 0.62 (theoretical value is 0.68. The weak hydroxyl peak near 3480 cm^{-1} indicating that the phenolic hydroxyl group was not reacted completely).

The infrared spectra of UiO-66 as shown in Fig. 4. The intense and broad characteristic peak at 3369 cm^{-1} due to the intercrystalline water and the physisorbed water condensed inside the cavities. The characteristic peaks at 1581 and 1398 cm^{-1} can be assigned to asymmetric and symmetric tensile vibration of O-C-O, respectively. The characteristic peak at 1506 cm^{-1} belong to the C = C in the benzene ring. In addition, the presence of the characteristic peak at 1660 cm^{-1} indicates the presence of DMF in the framework of UiO-66. The characteristic peak at 1100 cm^{-1} belong to the stretching vibration peak of the skeleton Zr-O single bond of UiO-66. The peaks at 823, 745, and 666 cm^{-1} are due to OH and C-H vibration in the terephthalic acid ligand. At lower frequencies, the characteristic peaks of Zr-O overlap with OH and C-H flexural vibration peaks (the main bands are 745, 666, 552, and 487 cm^{-1}, respectively) [21].

3.2 X-ray diffraction analysis

The X-ray diffraction spectrum of UiO-66 and its simulated are shown in Fig. 5.The X-ray diffraction spectrum of UiO-66 shows diffraction peaks at 2θ = 7.3°, 8.5°, 12.0°, 17.1°, 22.2°, 25.7°, which corresponding to crystal planes of (111), (002), (022), (044), (115) and (006), respectively.The peak

shape, peak intensity and position of UiO-66 are agreement with the results reported in reference 20. These evidences indicate that the UiO-66 with regular structure was successfully synthesized.

3.3 Dynamic mechanical properties analysis

The internal friction factor (Tan δ) and storage modulus (E´) of each sample are shown in Fig. 6. The maximum value of internal friction peak (Tan δ_{max}), crosslink density (V_e) and glass transition temperature (T_g) of each sample are shown in Table 2.

The V_e (sum of chemical crosslink and physical crosslink) could be obtained according to reference 23.

As seen from Fig. 6 (a), the Tan δ_{max} of NER/UiO-66 composites are much lower than that of sample P. Tan δ is the ratio of loss modulus to storage modulus. Under the same condition, the lower the Tan δ_{max} is the less internal loss of the material. Furthermore, the peak width at half-height of Tan δ for NER/UiO-66 composites is much broader than that of sample P, indicating the lower segmental mobility in the NER/UiO-66 composites. This is because NER matrix contains more epoxy functional groups than DGEBA, and its crosslink density after curing is much higher than that of DGEBA. UiO-66 contains polar carbonyl groups, which can make it partial compatible with epoxy resin matrix. On the other hand, UiO-66 as a rigid particle has a large steric effect. Therefore, the crosslink density of NER/UiO-66 composites decreased with increasing UiO-66 content, while the internal friction increased slightly with increasing UiO-66 content. When the content of UiO-66 is not higher than 3%, UiO-66 has good compatibility with NER, the storage modulus and T_g of NER/UiO-66 composites both increased with increasing UiO-66 content. When the content of UiO-66 is higher than 3%, the compatibility of UiO-66 and epoxy resin matrix begin to deteriorate, resulting in the decrease of storage modulus and T_g.

Table.2 Tan δ_{max}, V_e and T_g of each sample

Sample	P	A0	A1	A2	A3	A4	A5
Tan δ_{max}	1.032	0.155	0.168	0.178	0.187	0.207	0.212
V_e/(kmol/m^3)	9.19	146.19	84.19	82.74	71.08	55.60	52.95
T_g(℃)	53	154	169	172	178	165	164

3.4 Mechanical Properties Analysis

The impact strength of each sample is shown in Fig. 7. Proper crosslink density is beneficial to the improvement of polymer mechanical properties. The impact strength of sample A0 is 4.1 kJ/m^2, which is 2.0 kJ/m^2 higher than that of sample P. This is because the crosslink density of NER is higher than that of sample P (as shown in Table 2). The impact strength of NER/UiO-66 composites increased first and then decreased with increasingUiO-66 content. When the UiO-66 content is 4%, the impact strength of NER/UiO-66 composite (sample A4) is the maximum, which is 3.5 kJ/m^2 higher than that of pure

naringenin epoxy resin (sample A0). UiO-66 contains carbonyl groups, which makes it partially compatible with naringenin epoxy resin matrix when its content is not high. When the NER/UiO-66 composite is subjected to an external force, UiO-66 can induce and terminate the crazing, thereby exerting a toughening effect [22]. However, when the content of UiO-66 exceeds 4%, defects appear in NER/UiO-66 composites due to its agglomeration, which leads to the decrease of impact strength. This phenomenon is consistent with the dynamic mechanical properties discussed above.

3.5 Morphology analysis

Figure 8 shows the impact cross section of different samples. It can be seen from the figure that the cross section of sample P and A0 are smooth and show the characteristics of brittle fracture. The section of sample A4 is relatively rough, and many wrinkles can be observed, indicating that the material absorbs a lot of energy when subjected to external forces, which corresponds to its high impact strength. The cross section of sample A5 is smooth and some particles can be observed. This is due to the agglomeration of uio-66, resulting in defects in the material, which reduces the impact strength.

3.6 Thermal stability analysis

The thermal degradation curves of different samples are shown in Fig. 9. As shown in the figure, NER/UiO-66 composites have only one degradation stage. It shows that the addition of UiO-66 did not change the thermal degradation process of naringenin epoxy. The initial thermal degradation temperature (T_{d5}, Temperature at 95% mass retention rate [24]) of samples P and A series samples are 314 ℃, 316 ℃, 314 ℃, 302 ℃, 308 ℃, 297 ℃, and 299 ℃, respectively. The T_{d5} of NER/UiO-66 composites decreased with the increasing UiO-66 content. This is consistent with their crosslink density. It is noted that the residual char of NER/UIO-66 composite at 800 ℃ is significantly higher than that of DGEBA. This is because the higher the crosslink density, the easier it is to form a continuous dense char layer. The char formation will insulate the polymer-air interface, reduce the heat conduction, and starve the combustion process of decomposition products.

3.7 Limiting oxygen index analysis

The Limiting oxygen index (LOI) of sample P and A series samples are 21.0%, 22.2%, 23.3%, 23.6%, 23.8%, 24.5%, 24.5%, respectively. Since no flame-retardant fillers or elements are added to the samples, the improvement of LOI is not very significant. UiO-66 can promote the formation of char layer, thereby producing a thermal insulating layer and playing an auxiliary flame-retardant effect [19]. Thus, the LOI of NER/UiO-66 composites increased with increasing UiO-66 content.

4 Conclusions

The novel naringin epoxy resin was successfully synthesized. Maleic anhydride was used as curing agent, the impact strength and glass transition temperature of cured naringin epoxy resin were significantly higher than that of DGEBA. Naringin epoxy resin can be used as one of the alternatives to DGEBA. Low addition of UiO-66 can improve the mechanical properties and flame retardancy of naringin

epoxy resin at the same time. UiO-66 can be used as high-efficiency impact modifier and auxiliary flame retardant for rigid bio-based epoxy resin.

Declarations

Acknowledgements

This work was supported by the Natural Science Foundation of Hebei Province (No: B2019210221); S&T Program of Hebei (No: 206Z1202G); Postgraduate Innovation Project of Shijiazhuang Tiedao University (YC2021065).

References

1. P.Y. Jia, Y.F. Ma, Q.Y. Kong, L.L. Xu, Q.G. Li, Y.H. Zhou, Green Mater. **8**,6 (2020)
2. Y.G. Du, Y.M. Wang, Y.R. Yu, G.H. Shi, S. Zhou, M. Liu, S.T. Ren, X.X. Jia, G. Zhao, Poly. Bull. doi.org/10.1007/s00289-021-03616-x, (2021)
3. Liu Q Y, Wang D H, Li Z K, et al. Q.Y. Liu, D.H. Wang, Z.K. Li, Z.F. Li, X.L. Peng, C.B. Liu, Y. Zhang, P.L. Zheng, Mater. **13**, 2145 (2020)
4. T. Thakur, S. Jaswal, S. Parihar, B. Gaur, A. S. Singha, Express Polym. Lett. **14**, 512 (2020)
5. C. Gioia, M. Colonna, A. Tagami, L. Medina, O. Sevastyanova, L. A. Berglund, M. Lawoko, Biomacromolecules **21**, 1920 (2020)
6. T.N. Tran, C. Di Mauro, A. Graillot, A. Mija, Macromol. **53**, 2526 (2020)
7. X. Zhen, H.W. Li, Z.B. Xu, Q.F. Wang, S.N. Zhu, Z.M. Wang, Z.H. Yuan, Int. J. Biol. Macromol. **182**, 276 (2021)
8. D.J. Van De Pas, K.M. Torr, Biomacromolecules **18**, 2640 (2017)
9. T.T. Li, X.Q. Liu, Y.H. Jiang, S.Q. Ma, J. Zhu, Iran. Polym. J. **25**, 957 (2016)
10. A.L. Brocas, A. Llevot, C. Mantzaridis, G. Cendejas, R. Auvergne, S. Caillol, S. Carlotti, H. Cramail, Des. Monomers Polym. **17**, 301 (2013)
11. C. Mantzaridis, A.L. Brocas, A. Llevot, G. Cendejas, R. Auvergne, S. Caillol, S. Carlotti, H. Cramail, Green Chem. **15**, 3091(2013)
12. E. Kinaci, E. Can, J.J.L. Scala, G.R. Palmese, Polym. **12**, 1956 (2020)
13. S.P. Huo, H.L. Ma, G.F. Liu, C. Jin, J. Chen, G.M. Wu, Z.W. Kong, ACS Omega **12**, 16403 (2018)
14. J.Y. Dai, Y.Y. Peng, N. Teng,Y. Liu, C.C. Liu, X.B. Shen, S. Mahmud, J. Zhu, ACS Sustain. Chem. Eng. **6**, 7589 (2018)
15. N. Domun, H. Hadavinia, T. Zhang, T. Sainsbury, G.H. Liaghat, S. Vahid, Nanoscale **7**, 10294 (2015)
16. S.E. Bambalaza, H.W. Langm, R. Mokaya, N.M. Musyoka, L.E. Khotseng, ACS Appl. Mater. Interfaces **12**, 24883(2020)

17. Z.P. Smith, J.E. Bachman, T. Li, B. Gludovatz, V.A. Kusuma, T. Xu, D.P. Hopkinson, R.O. Ritchie, J.R. Long, Chem. Mater. **30**, 1484 (2018)
18. H.Z. Liu, H. Peng, Y.M. Xin, J.Y. Zhang, Polym. Chem. **10**, 2263 (2019)
19. Chen W L, Jiang Y, Qiu R, et al. W.L. Chen, Y. Jiang, R. Qiu, W. Xu, Y.B. Hou, Macromol. Res. **28**, 42 (2020)
20. J.H. Cavka, S. Jakobsen, U. Olsbye, N. Guillou, C. Lamberti, S. Bordiga, K.P. Lillerud, J. Am. Chem. Soc. **130**, 13850 (2008)
21. C.Q. Chen, D.Z. Chen, S.S. Xie, H.Y. Quan, X.B. Luo, L. Guo, ACS Appl. Mater. Interfaces **9**, 4104 3(2017)
22. C. Hu, J.D. Xiao, X.D. Mao, L.L. Song, X.Y. Yang, S.J. Liu, Mater. Lett. **240**, 113 (2019)
23. L. Lin, H. Zhang, Y. Li, H. Zhang, China Thermosetting resin **27**, 60 (2012)
24. X.P. Xu, S. Chen, W. Tang, Y.J. Qu, X. Wang, Polym. Degrad. Stab. **98**, 659 (2013)

Figures

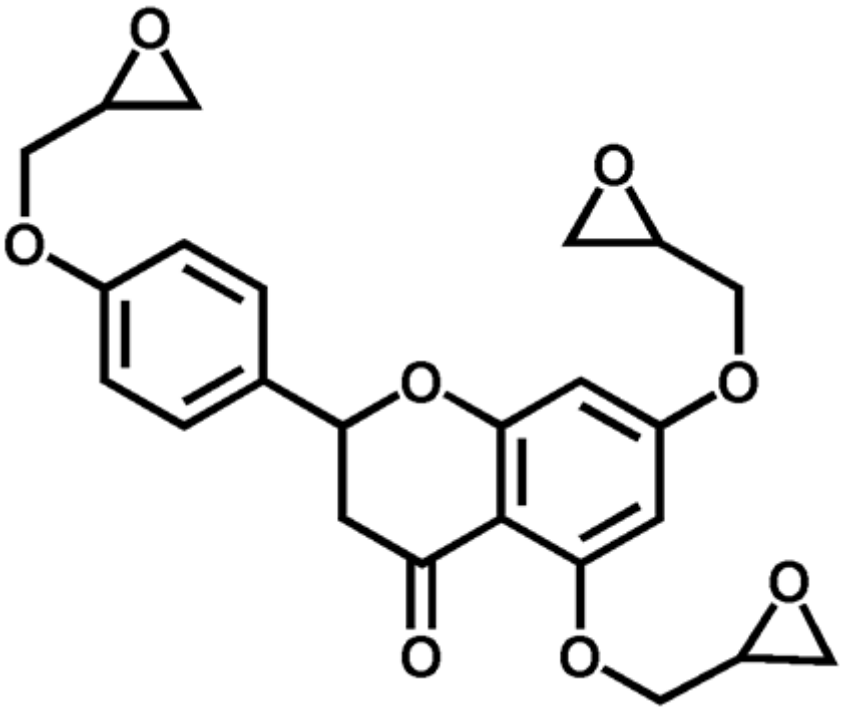

Figure 1

structure of naringenin epoxy resin matrix

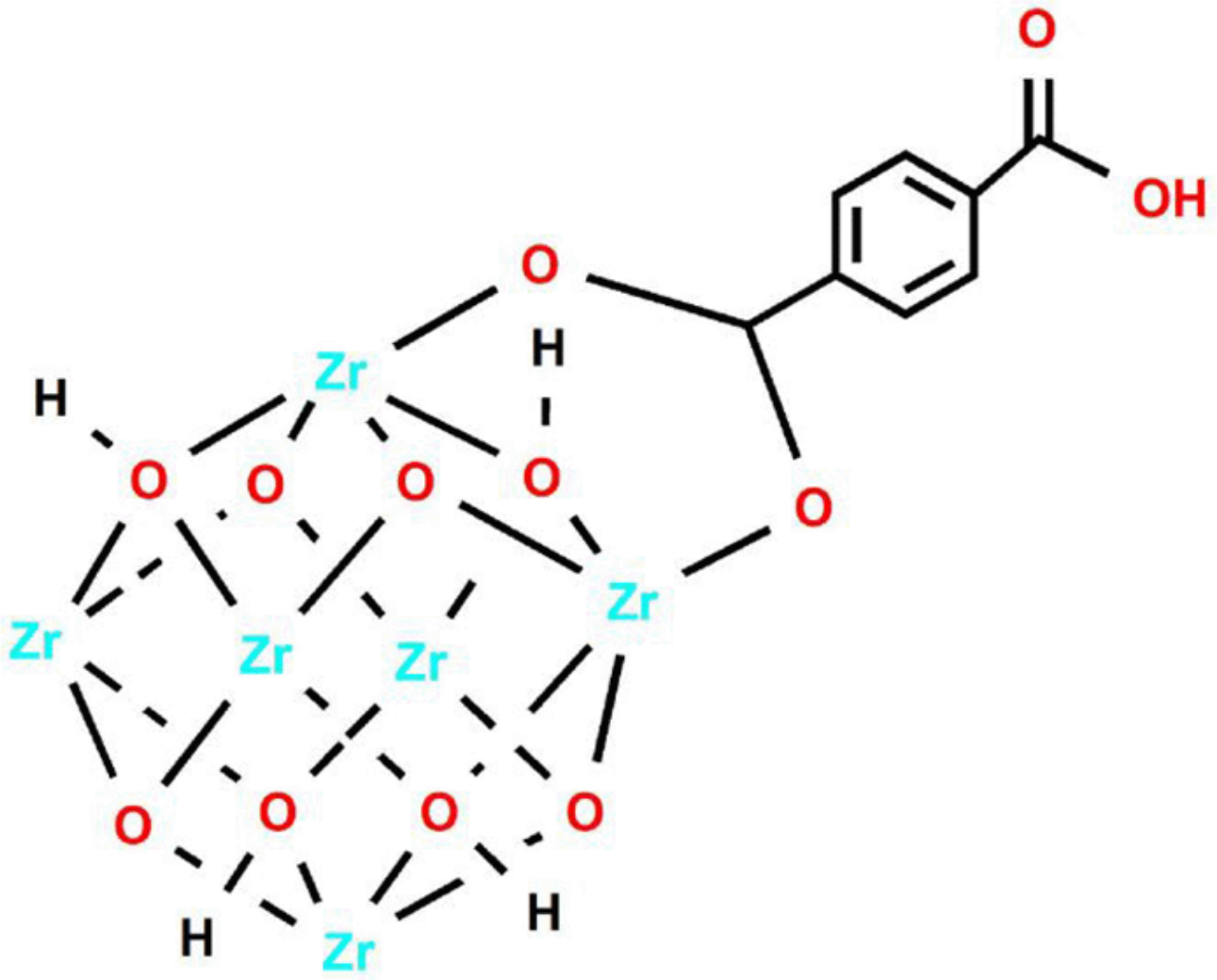

Figure 2

Structure of UiO-66

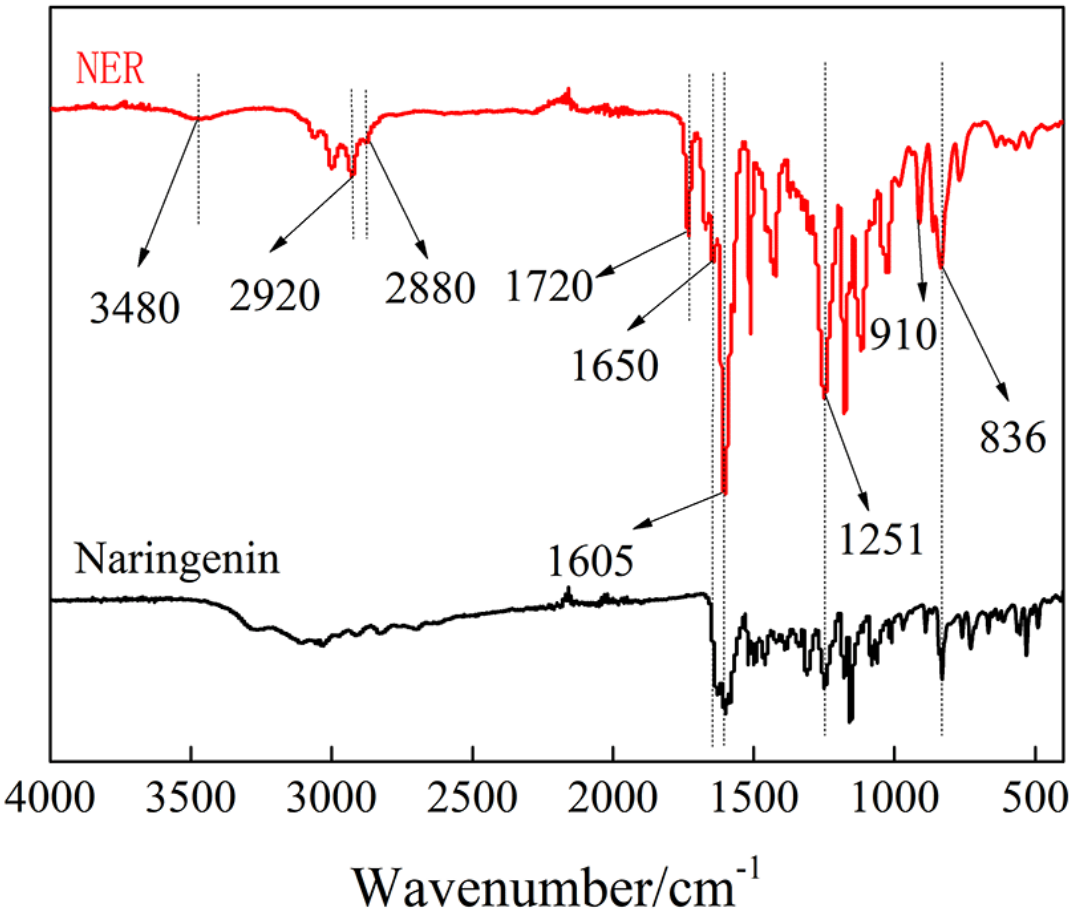

Figure 3

The infrared spectra of naringenin and NER

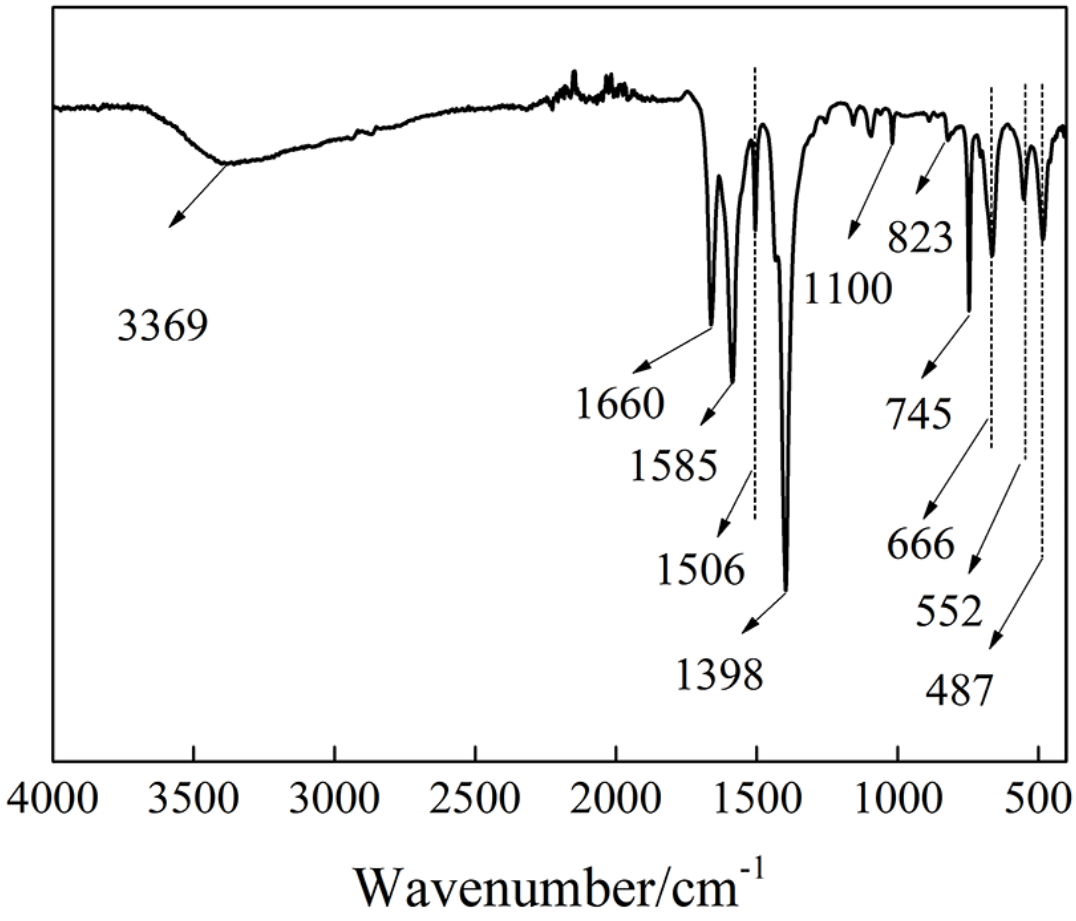

Figure 4

The infrared spectra of UiO-66

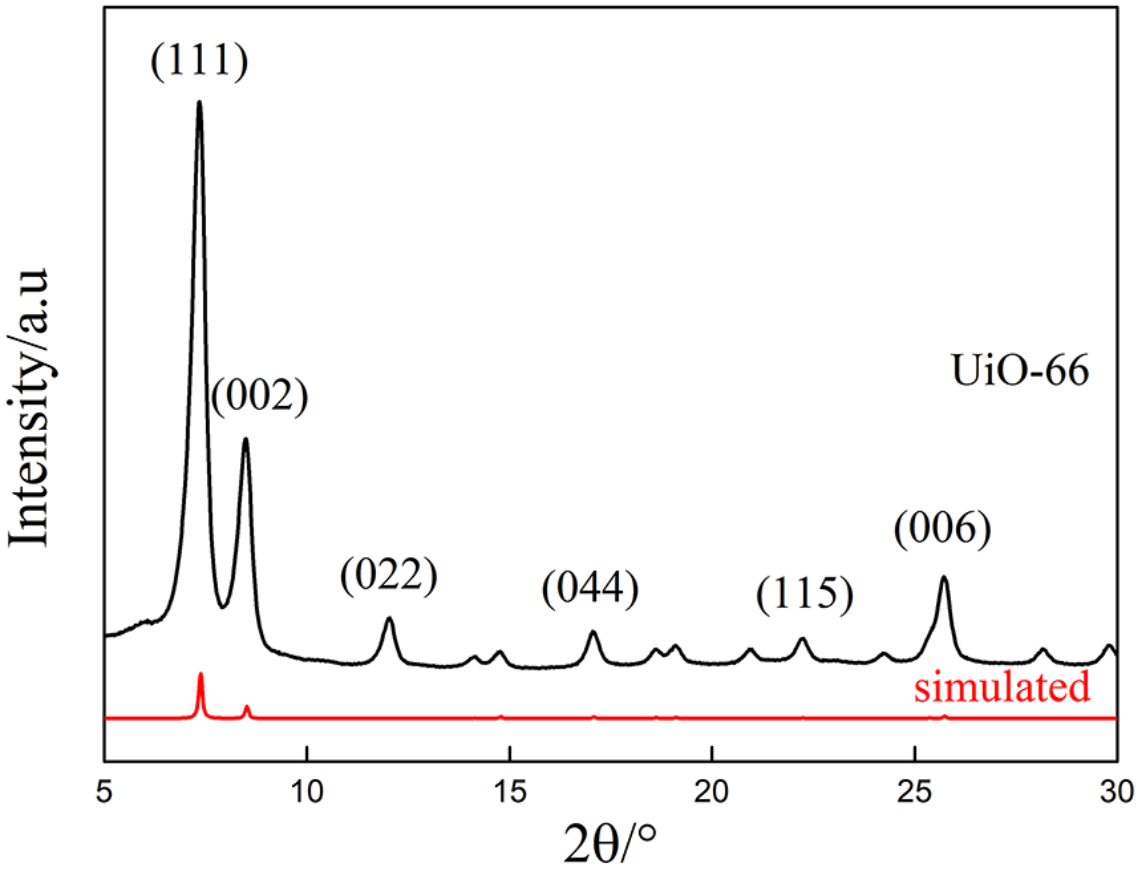

Figure 5

The X-ray diffraction spectrum of UiO-66 and its simulated

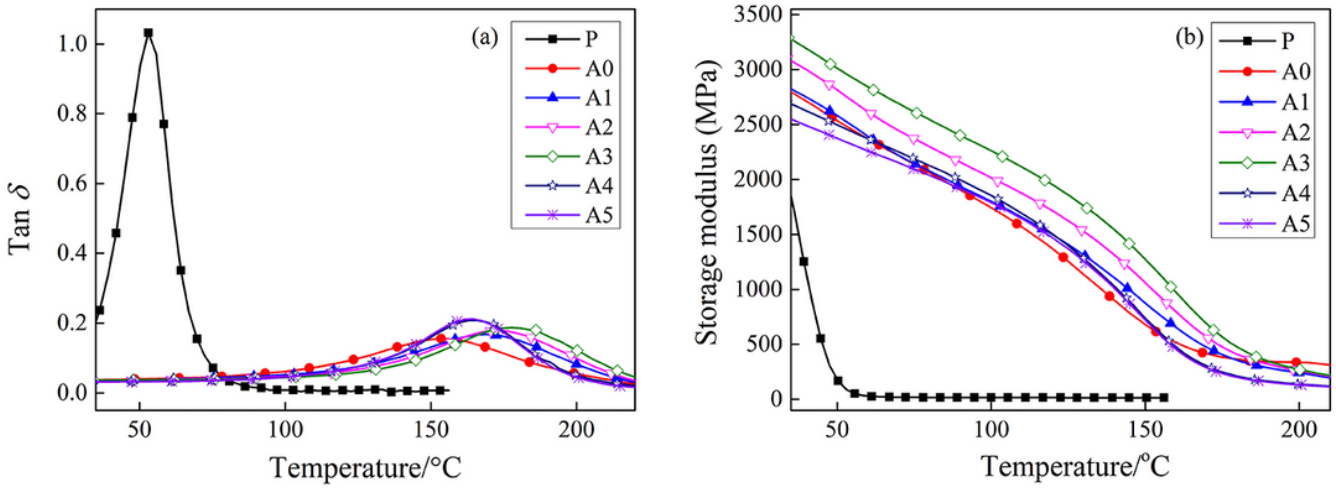

Figure 6

Tan δ and storage modulus of different samples (a) Tan δ (b) Storage modulus

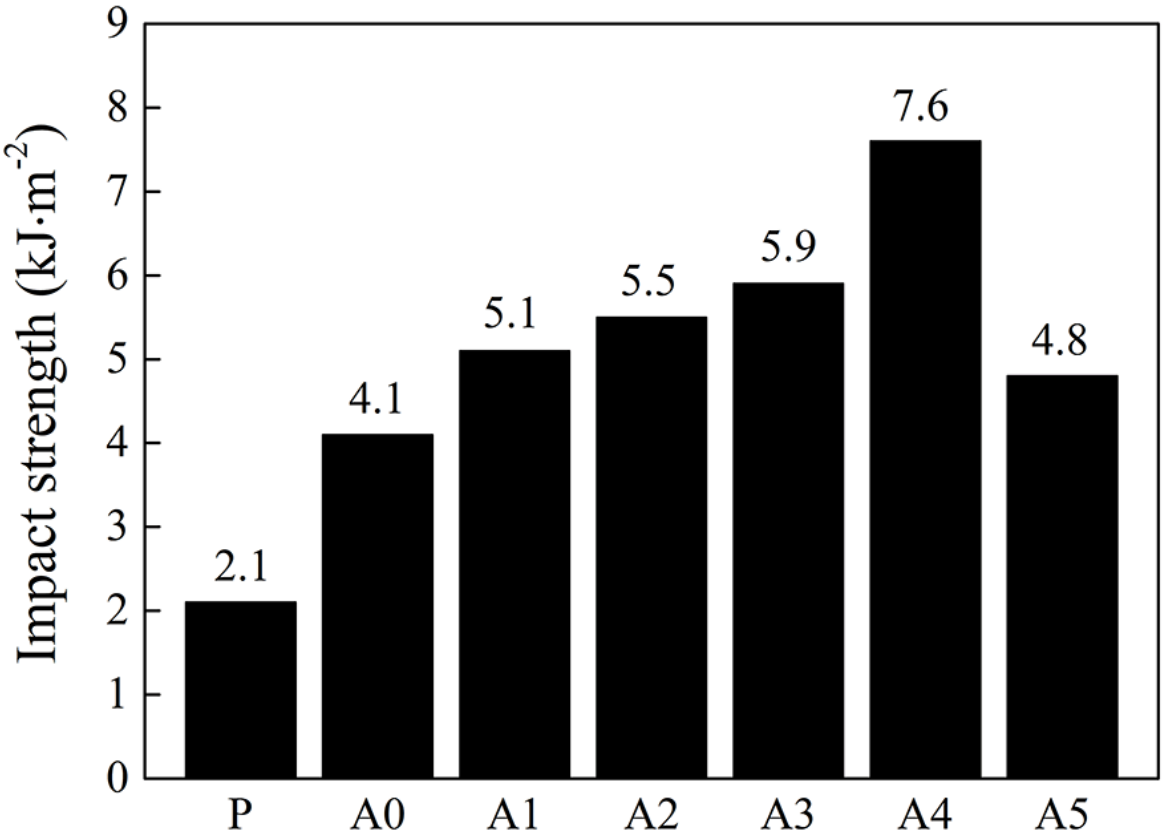

Figure 7

Impact strength of each sample

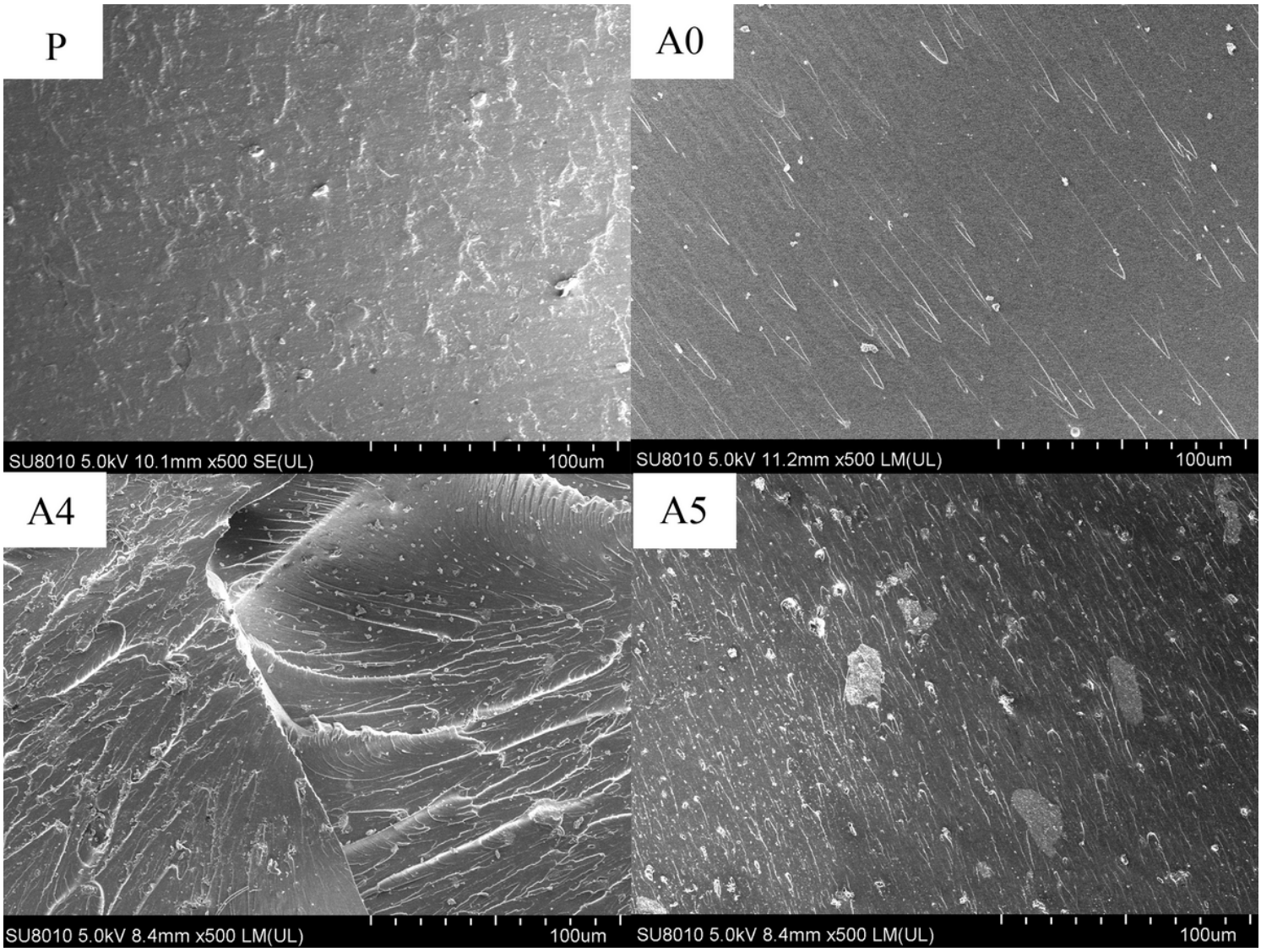

Figure 8

The impact cross-section SEM images of different samples

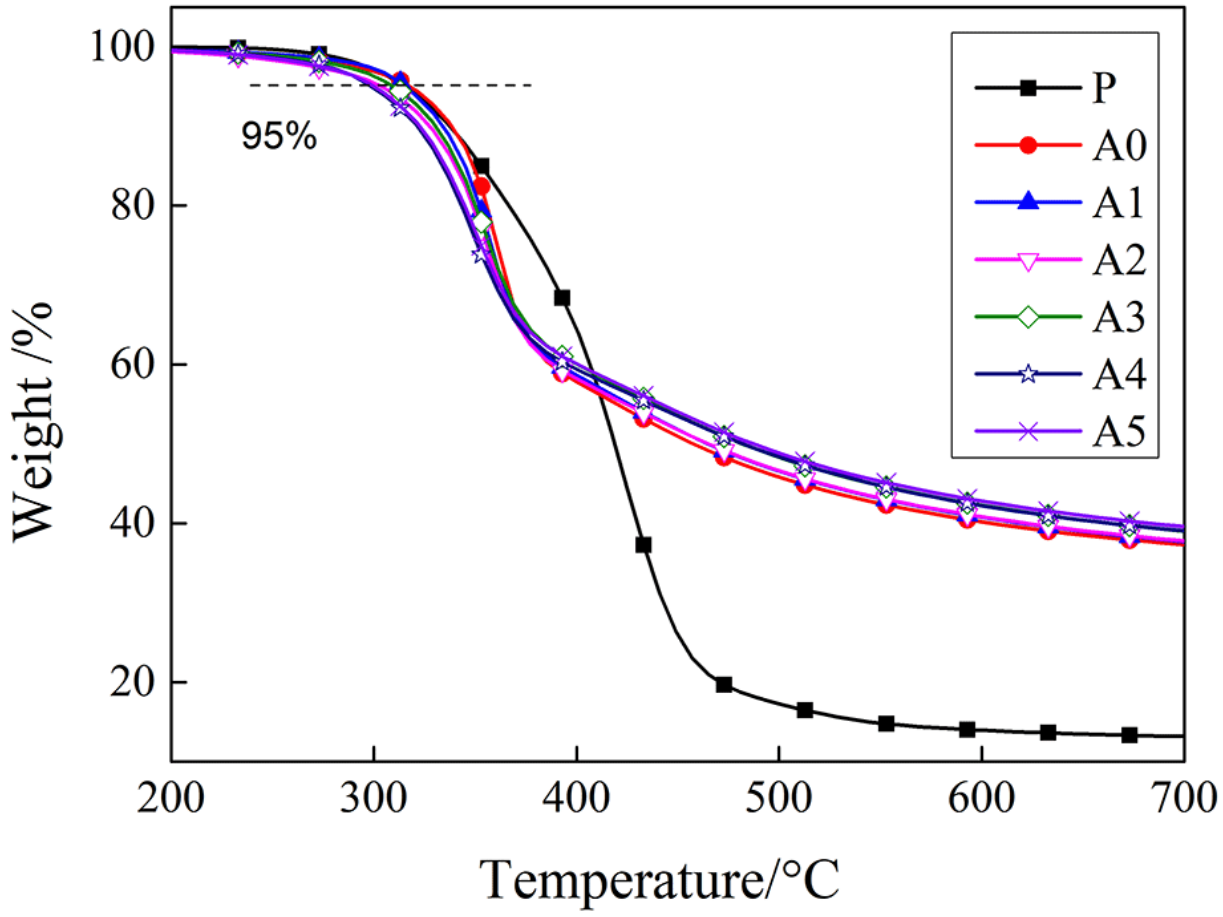

Figure 9

Thermal degradation curves of different samples